Preprints of the 19th World Congress
The International Federation of Automatic Control
Cape Town, South Africa. August 24-29, 2014

Position-Dependent Repetitive Control for Speed Ripple Reduction of Ultrasonic Motor

Chun-Lin Chen and Mi-Ching Tsai*

**Department of Mechanical Engineering, National Cheng Kung University, Tainan 701, Taiwan*
(Tel: +886-6-2757575 ext. 62173; e-mail: mctsai@mail.ncku.edu.tw).

Abstract: Ultrasonic motors are driven by the friction force between the rotor and the vibrator, which often induces speed fluctuations synchronizing with the rotor position periodically, namely, speed ripples. This paper employs the plug-in type repetitive control for rejecting the position-dependent periodic speed ripple and presents an implementation technique based on rotor position information. A mathematical description for characterizing the speed ripple is introduced using the Fourier series. A position-dependent repetitive controller design and an interpolation scheme to manipulate the delayed data based on the acquired rotor position are developed to improve control performance in speed ripple reduction. Simulation and experimental results are given to confirm the validity of the proposed repetitive control design and implementation.

Keywords: Speed Control, Speed Ripple, Repetitive Controller

1. INTRODUCTION

Ultrasonic motors (USMs) have many beneficial features, such as self-locking when unexcited, quick response, quiet operation, and no electromagnetic interference. A USM is composed of a vibrator and a rotor in which the rotor is driven through the friction force by the ultrasonic vibration of the vibrator. However, the inherent problem of USMs, speed fluctuation, synchronizes with the rotor position periodically. The dynamic modelling of USMs can be found in the literature (Ming *et al*., 2001). Speed control of USMs by adaptive control (Senjyu *et al*., 1994), fuzzy logical control (Sun *et al*., 2007), neural networks (Xu *et al*., 2005), and hybrid control have been investigated, respectively. It is known that the fluctuation of revolving speed, namely, speed ripple, appears inherently by the driving structure of USMs.

To supress the inherent speed ripples, a PI-repetitive controller was proposed by Senjyu (Senjyu *et al*., 1995) and a controlled system with adjustable driving frequency and driving voltage was developed (Izuno *et al*., 1998). A robust H_∞ control design (Kobayashi *et al*., 1999) and a zero phase error tracking controller (ZPETC) (Rodriguez *et al*., 2000) can be incorporated with a repetitive controller for speed control. In this paper, the speed ripples are characterized by the Fourier series and the plug-in type repetitive control, proposed by Tsai (Tsai *et al*., 2002) and Chen (Chen *et al*., 2013), is employed to design the speed controller.

2. ULTRASONIC MOTOR

Consider the rotary type of USMs with asymmetrical driving electric fields (VAEF), which is fixed by a certain preload generated by a compressed spring. This USM, which was developed in the previous work (Hsiao *et al*., 2010), has a single-phase drive and a vibrator.

When the driving voltage is applied to the VAEF, the vibrator oscillates along an oblique line trajectory such that the rotor rotates in the direction of the friction force. A prototype of the motor used in the experimental setup, which consists of a load cell, a shaft encoder, and a power amplifier, is illustrated in the experimental setup of Fig. 1. The specifications of the prototype motor are listed in Table I.

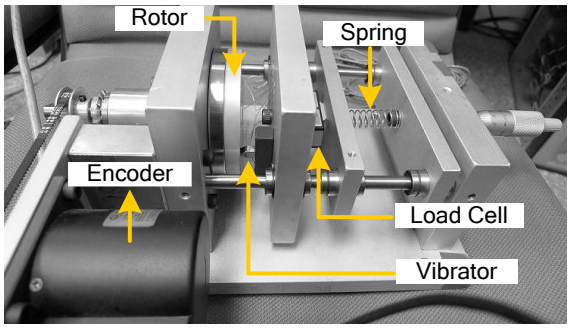

Fig. 1. Prototype of single-phase VAEF ultrasonic motor.

Table 1. Specifications of ultrasonic motor

Rotor	Aluminium ψ 82×H 10 mm
Piezoelectric ceramic	PZT-5H L 5×W 5×H 5 mm
Driving frequency	70 kHz
Driving voltage	68 V_{rms}
Max. revolving speed	120 rpm
Max. torque	10 N-mm

Both amplitude and frequency of the driving AC voltage can be utilized for speed control of the single-phase drive ultrasonic motor. The speed response of the ultrasonic motor is shown in Fig. 2 at the operating frequency of 70 kHz. As can be seen, the fluctuation phenomenon in the revolving

speed, i.e., speed ripple, emerges in the revolving speed. Since the speed ripple is caused by the irregularities in the contacting surface, the period of the speed ripple is synchronous to the angular position of the rotor. Let the motor operate at 60 rpm. It can be found in the frequency components from Fourier transform of Fig. 3 that there are some peaks occurring at $n \cdot \omega / 60$ Hz, where ω is the revolving speed and $n = 1, 2, 3, \ldots$. For the case of $\omega = 60\,rpm$, these peaks occurred at 1, 2, 3…Hz. The speed ripple ranges from 3 to 6 rpm as can be seen from Fig. 2.

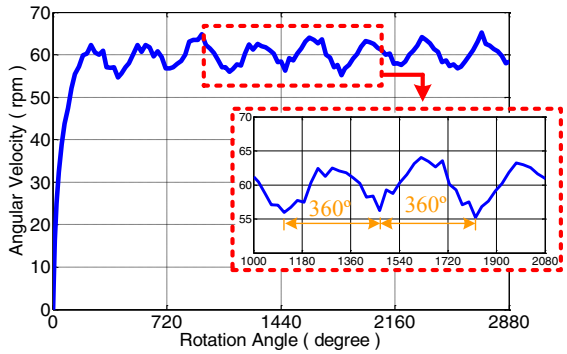

Fig. 2. Revolving speed response according to rotor position

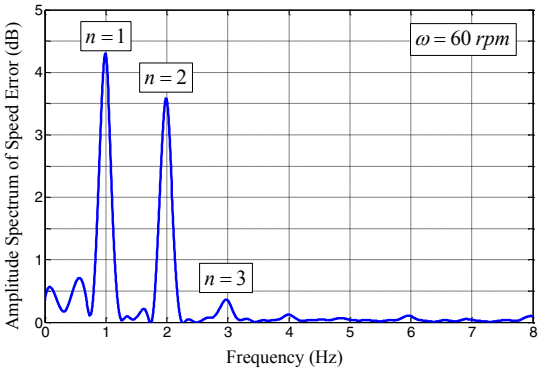

Fig. 3. Frequency components of speed ripple.

3. MODELING OF SPEED CHARACTERISTICS

To deal with the inherent nonlinearity of USMs for speed control, this paper proposes a repetitive controller design to reduce these ripples. Fig. 4 shows a block diagram of the ultrasonic motor from the input driving voltage V_{dri} to the output revolving speed ω_R, where $G(s)$ denotes a nominal model of the ultrasonic motor, ω_R^* indicates the revolving speed without the speed ripple, and ω_D represents the speed ripple. As studied by Nakamura (Nakamura *et al.*, 1991), a model of the ultrasonic motor with linear load characteristics can be simplified as a first-order system for speed controller design. The system parameters are obtained, by the measured speed responses shown in Fig. 5 as,

$$G(s) = \frac{K}{\tau s + 1} = \frac{0.29}{0.25 s + 1}, \qquad (1)$$

where $K = 0.29$ is the dc gain and $\tau = 0.25$ is the time constant.

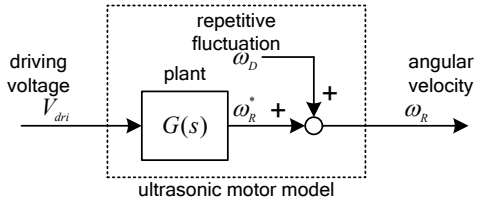

Fig. 4. Model of ultrasonic motor.

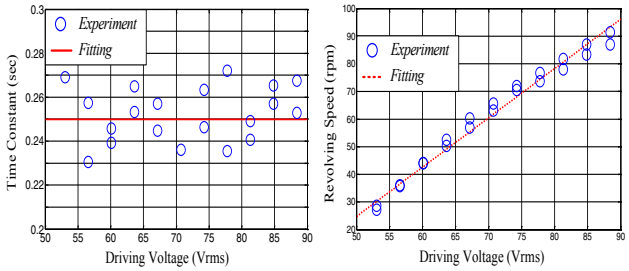

(a) Time Constant (b) DC Gain

Fig. 5. Fitting for ultrasonic motor.

Let ω_D be periodic and synchronous to the rotor position θ, given by

$$\omega_D(\theta) = A + B_1 \sin(\theta + \phi_1) + B_2 \sin(2\theta + \phi_2) + \ldots + B_n \sin(n\theta + \phi_n). \qquad (2)$$

Note that the parameters of the Fourier series, A, B_n, and ϕ_n, can be found from the experimental data of measured speed responses by curve fitting. Let the fitting error be defined as:

$$e_{fit} = \hat{\omega}_D(\theta) - \omega_D(\theta), \qquad (3)$$

where $\hat{\omega}_D$ and ω_D denote the speed ripples from the experimental data and the proposed model, respectively.

It can be observed in Fig. 6 that the Fourier series not only satisfies the continuity at $\theta = 0$ and 2π, but also matches the experimental data closely in which the fitting error is bounded within ±2 rpm. To validate the accuracy of the identified model, the model output is compared with the actual measured speed responses, which result from different driving conditions as shown in Fig. 7. The revolving speed obtained from the identified model has good agreement with the actual speed responses in each driving condition.

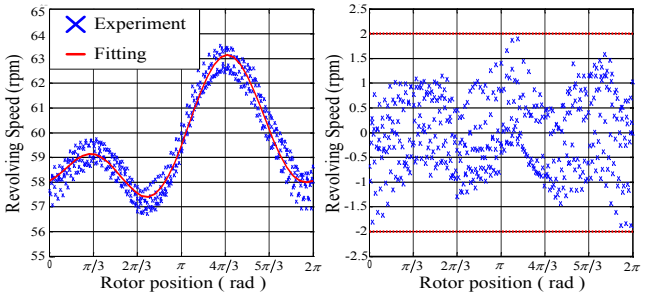

(a) Revolving Speed (b) Fitting Error

Fig. 6. Fitting for position-dependent speed ripple of USMs.

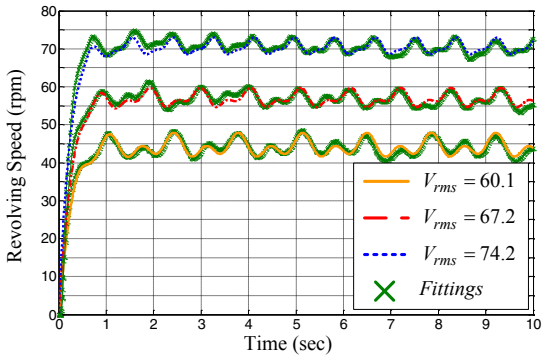

Fig. 7. Comparisons of estimated and actual revolving speed.

4. SPEED CONTROL OF USM

Consider the speed control system of the USM shown in Fig. 8, where $C(s)$ is the PI controller in that K_P and K_I are the proportional and integral gains, respectively. Let ω^* denote the speed command, ω the rotor speed, and e_{PI} the corresponding speed error.

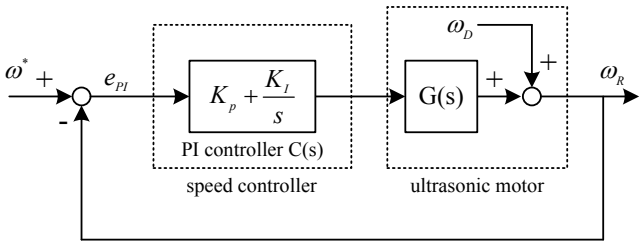

Fig. 8. Block diagram of USMs with PI controller.

For constant speed operation, the rotor position will satisfy $\theta = \omega^* t$. The speed ripple synchronous to the rotor position can be rewritten as

$$\omega_{Dm}(t) = A + B_1 \sin(\omega^* t + \phi_1) + B_2 \sin(2\omega^* t + \phi_2) + \ldots + B_n \sin(n\omega^* t + \phi_n). \quad (2)$$

Then, e_{PI} in Fig. 8 is given by

$$e_{PI}(s) = \frac{1}{1+G(s)C(s)}(\omega^* - \omega_D) = S_0(s)(\omega^* - \omega_D). \quad (4)$$

Equation (4) implies that the speed error e_{PI} could remain significant due to the periodic speed ripple of ω_D since the large loop gain in practical implementation will saturate the actuator, creating instability.

In general, the speed ripple could be considered as the time-dependent periodical disturbance for constant speed operation. To attenuate the influence of ω_D with the period of T_D, the plug-in type repetitive controller can be employed to the PI control system as shown in Fig. 9, where the low-pass filter K_q can be designed to eliminate the period error of e_R. Note that the controller $C(s)$ of Fig. 9 must be designed properly to ensure that the closed loop system without the repetitive controller is internally stable.

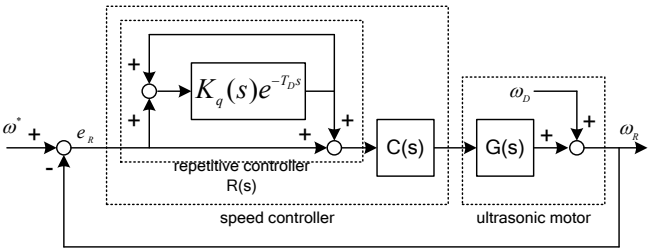

Fig. 9. Block diagram of speed control with repetitive controller.

For the repetitive control system of Fig. 9, two design conditions are required to guarantee that the speed control system is internally stable.

Condition 1)
The closed-loop system without the repetitive controller is internally stable

Condition 2)
$$|K_q(j\omega)| < |1 + GC(j\omega)| \quad \forall \omega \in \Re$$

Now e_R of the repetitive control system is determined by

$$e_R = \frac{1}{1+R(s)C(s)G(s)}(\omega^* - \omega_D) = S_0(1 - K_q e^{-T_D s})(\frac{1}{1 - S_0 K_q e^{-T_D s}})(\omega^* - \omega_D), \quad (5)$$

where $R(s)$ is defined by

$$R(s) = (1 - K_q(s)e^{-T_D s})^{-1}. \quad (6)$$

For satisfying *Condition 2*), let (6) be rewritten as

$$e_R(s) = e_{R\_0}(s) + e_{R\_1}(s) + e_{R\_2}(s) + \ldots + e_{R\_k}(s) \quad (7)$$

and

$$e_{R\_k}(s) = (1 - K_q e^{-T_D s}) S_0^{k+1} K_q^k e^{-kT_D s}(\omega^* - \omega_D), \quad (8)$$

where k represents the *k-th* period of ω_D. Let e_{R_k} be further expressed as

$$\left\| \frac{e_{R\_k}}{e_{R\_k\text{-}1}} \right\|_2 = \left\| S_0 K_q e^{-T_D s} \right\|_2 = \left\| S_0 K_q \right\|_2 < 1. \quad (9)$$

Therefore, (8) can be extended as

$$e_R(s) \cong e_{PI}(s) - [S_0(1-S_0)K_q e^{-T_D s} + S_0^2(1-S_0)K_q^2 e^{-2T_D s} + S_0^3 K_q^3 e^{-3T_D s}](\omega^* - \omega_D) = e_{PI}(s) - \hat{e}(s). \quad (10)$$

Obviously, (9) concludes that the speed error e_R converges gradually after the first period of ω_D such that $\hat{e}$ will track e_{PI} as time increases as shown in Fig. 10. This leads to the

superior reduction of speed ripple with the repetitive controller.

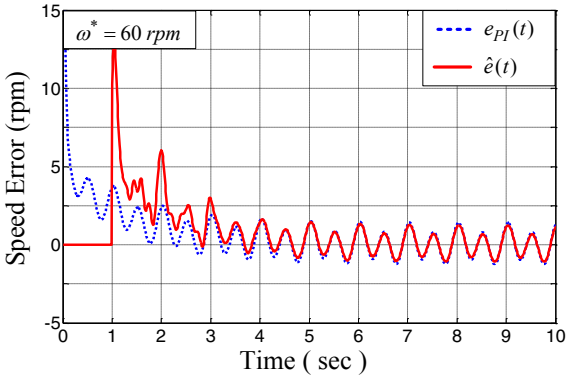

Fig. 10. Comparison of speed error components with repetitive controller: e_{PI} and $\hat{e}$.

5. EXPERIMENTS

To demonstrate the effectiveness of the proposed control method, the speed responses are compared with the two control systems, i.e., only PI controller and PI controller with the repetitive controller. In addition to the conventional time-dependent repetitive controller, this paper also presents an implementation based on the rotor position. This position-dependent repetitive controller could suppress the time varying periodic problem effectively.

5.1 Implementation of Time-Dependent Delay

The implementation of the time delay is a crucial technique in the repetitive controller, which is responsible for the release time of the control effort from the repetitive controller. A time delay unit is shown in Fig. 11. The data of speed error e_R should be stored in the buffer in succession, and then the delayed data is released after a designed delay time, i.e., one period of the speed ripple. The time-dependent repetitive control for speed ripple reduction can be found in our previous work (Chen et al., 2013). However, the period of speed ripple often varies as shown in Fig. 12. Let the mathematical description for the speed ripple be modified as

$$\hat{\omega}_{Dm}(t) = A + B_1 \sin(\omega^* t + \phi_1) + B_2 \sin(2\omega^* t + \phi_2) + \Delta . \quad (11)$$

According to the uncertainty in the practical operation, the speed ripple behaves as a time varying periodic but is still a position dependent signal. The delay unit in the repetitive controller, therefore, should be modified.

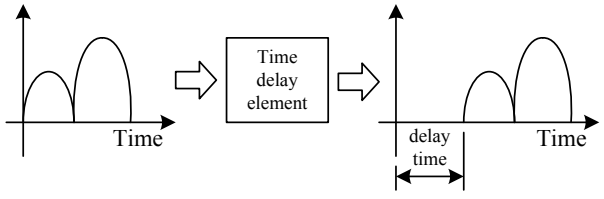

Fig. 11. Function of time delay unit.

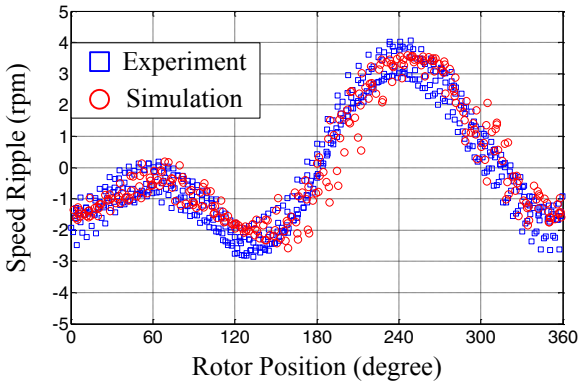

Fig. 12. Model uncertainty and time variant period of speed ripple.

5.2 Implementation of Position-Dependent Delay

The position-dependent delay is implemented in order to properly access the stored data in buffer for the repetitive controller, for the case of a time varying periodic signal but position-dependent as in Fig. 13. The times between each measured data point of the time-varying periodic signal with a fixed sampling rate are different.

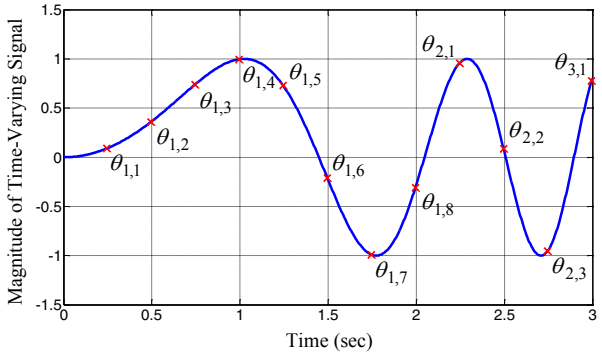

Fig. 13. Time-varying periodic signal with fixed sampling rate.

The proposed technique in this paper is to use the information of rotor position to manipulate the delayed unit in the buffer. The $j-th$ measured rotor position in the $i-th$ revolution of the rotor is represented as $\theta_{i,j}$, where $j = 1, 2, 3, ..., k_i$. For the case of a time periodic signal, the measured number j and the measured rotor position $\theta_{i,j}$ should be the same, i.e., $k_1 = k_2 = k_i$ and $\theta_{1,j} = \theta_{2,j} = \theta_{i,j}$. However, if the period of the speed ripple is time-varying, it could be clearly found that $k_1 \neq k_2 \neq k_i$ and $\theta_{1,j} \neq \theta_{2,j} \neq \theta_{i,j}$. Therefore, a modified manipulation of the delayed data with respect to the rotor position is proposed in the following.

Consider the position-dependent delay unit in which the data is released in succession after a designed delay position period, i.e., one revolution of the rotor. According to the significant differences between the measured periods of the rotor positions in each revolution, an interpolation scheme is

developed to properly generate the delay signal with respect to the position information as

$$R(\theta_{i+1,\hat{j}}) = R(\theta_{i,j}) + \frac{R(\theta_{i,j+1}) - R(\theta_{i,j})}{\theta_{i,j+1} - \theta_{i,j}} \times (\theta_{i+1,\hat{j}} - \theta_{i,j}), \quad (12)$$

$$if\ \theta_{i,j} \le \theta_{i+1,\hat{j}} \le \theta_{i,j+1}$$

where $i \ge 1$ and $\theta_{1,0} = 0$

The advantage of the proposed delay technique in the repetitive controller is exported by the frequency components from the Fourier transform as shown in Fig. 14. For the case of the fixed time period of the speed ripple, the speed ripple reduction by both time-dependent and position-dependent delay approaches are almost the same because of $\theta = \omega^* t$. However, for the case of a non-fixed time period of the speed ripple, the speed ripple can be reduced significantly by the position-dependent repetitive controller.

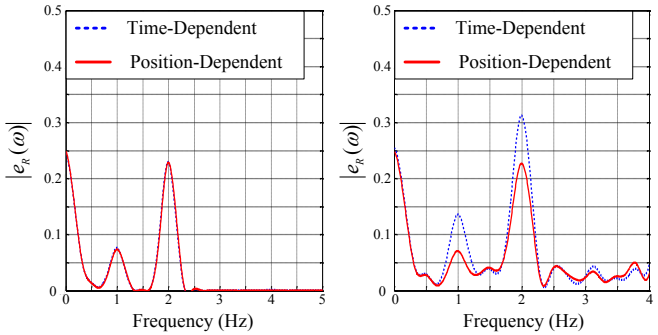

(a) Without uncertainty (b) With Uncertainty

Fig. 14. Comparison by frequency components for speed ripple reduction

5.3 Controller Performance Comparisons

To demonstrate the effectiveness of the proposed position-dependent repetitive controller, the experimental error responses and the frequency components from the Fourier transform are compared with that resulting from the other two control systems, i.e., the PI controller with and without the time-dependent repetitive controller. Note that the bandwidth ω_q of K_q must be designed to satisfy Condition 2) and also be higher than the bandwidth of ω_D as shown in Fig. 15. As can be seen in Fig. 15, the dotted and the dash lines represent $|1+GC(j\omega)|$ and the bandwidth of ω_D, respectively. The solid line is the plot of the first-order low-pass filter $|K_q(j\omega)|$. Nevertheless, the higher bandwidth of K_q leads to some noise problems in practical implementation.

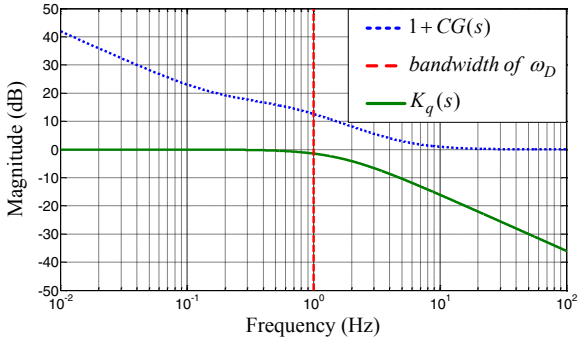

Fig. 15. Design restriction of low-pass filter K_q

Figure 16 shows the error responses and the frequency components resulting from the PI controller and the time-dependent repetitive controller, respectively, for the command speed $\omega^* = 60\,(rpm)$. The index to evaluate the effectiveness is defined as

$$index = \frac{\max(|\hat{\omega}_D'|)}{\max(|\hat{\omega}_D|)}, \quad (13)$$

where $\hat{\omega}_D$ is the speed ripple without controlling, and $\hat{\omega}_D'$ is the speed ripple resulting from utilizing the controllers previously addressed in this paper.

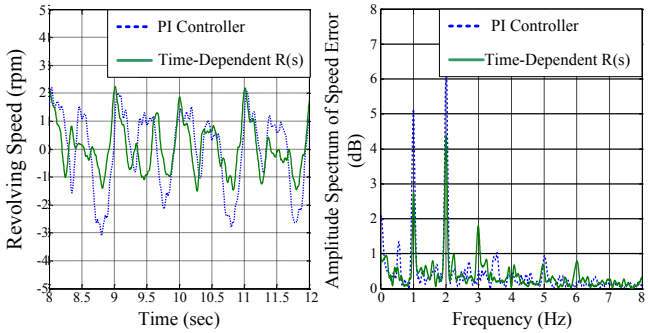

(a) Error response (b) Frequency components

Fig. 16. Comparison of control systems: PI controller and time-dependent repetitive controller.

Moreover, the control performance of the proposed position-dependent repetitive controller is compared with that of the time-dependent repetitive controller. The experimental result is shown in Fig. 17.

The comparisons of the three control systems addressed in this paper are depicted in Fig. 18, and the effectiveness of the speed ripple reduction was listed in Table 2. For the proposed repetitive controller, it can be found that the speed ripple is 45% of ω_D and 20% smaller than the time-dependent repetitive controller.

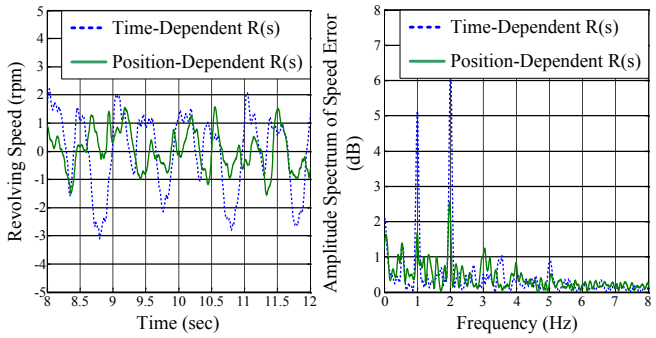

Fig. 17. Comparison of speed control: time-dependent and position dependent repetitive controllers.

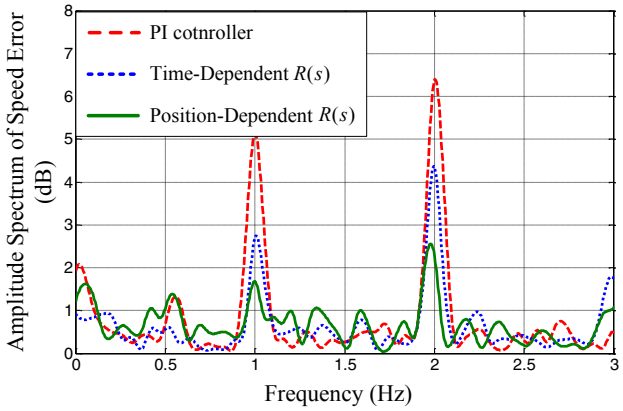

Fig. 18. Comparison of PI, time-dependent and position-dependent control systems.

Table 2. Effectiveness of speed ripple reduction

System	Speed Ripple (rpm)	Index (%)
open loop	7	
PI	5.87	83.8
Time-Dependent	4.51	65
Position-Dependent	3.12	45

6. CONCLUSION

This paper has investigated the speed control of a single-phase drive ultrasonic motor, which has inherent speed ripples. The model of speed ripples, described by the Fourier series, was adopted for designing the speed controllers of USMs. The repetitive controller exhibits the advantage of better speed ripple reduction than the PI controller system. An implementation of the delay unit based on the rotor position has been proposed in the repetitive controller. The superiority of the proposed technique is verified by reducing 55% of speed ripple and is 20% smaller than the conventional time-dependent implementation.

ACKNOWLEDGMENT

This work was supported by National Science Council (NSC) of Taiwan, under project NSC 102-2221-E-006-001.

REFERENCES

Chen, C.L., Tsai, M.C. and Hsiao, S.W. (2013). Repetitive controller for speed ripple reduction of ultrasonic motors. *Proceeding of International Conference on Automatic Control* (accepted).

Hsiao, S.W. and Tsai, M.C. (2010). Single-phase drive linear ultrasonic motor with perpendicular electrode vibrator. Japanese *Journal of Applied Physics*, vol. 49, pp. 024201-024201-7.

Izuno, Y. and Nakaoka, M. (1998). Speed tracking servocontrol system with speed ripple reduction scheme for traveling-wave-type ultrasonic motor. *Electronics and Communications in Japan*, Part 3, vol. 81, pp. 1-9.

Kobayashi, Y., Kimura, T. and Yanabe, S. (1999). Robust speed control of ultrasonic motor based on H^{∞} control with repetitive compensator. *Japan Society of Mechanical Engineers*, Series C, vol. 42, pp. 884-890.

Ming, Y. and Peiwen, Q. (2001). Performances estimation of a rotary traveling wave ultrasonic motor based on two-dimension analytical model. *Ultrasonics*, vol. 39, pp. 115~120.

Nakamura, K., Kurosawa, M., Kurebayashi, H. and Ueha, S. (1991). An estimation of load characteristics of an ultrasonic motor by measuring transient responses. *IEEE Transactions on Ultrasonics, Ferroelectrics and Frequency Control*, vol. 38, pp. 481-485.

Rodriguez, H., Pons, J.L. and Ceres, R. (2000). A ZPET-repetitive speed controller for ultrasonic motors. *Proceeding of International IEEE Conference on Robotics and Automation*, pp. 3654-3659.

Senjyu, T., Miyazato, H. and Uezato, K. (1994). Perofrmance comparison of PI and adaptive controller for adjustable speed drives of ultrasonic motors. *Proceeding of International Conference on Industrial Technology*, pp. 519-523.

Senjyu, T., Miyazato, H. and Uezato, K. (1995). Precise speed control of ultrasonic motors with repetitive control. *Proceeding of International IEEE Conference on Industrial Automation and Control*, pp. 165-169.

Sun, Z., Xing, R., Zhao, C. and Huang, W. (2007). Fuzzy auto-tuning PID control of multiple joint robot driven by ultrasonic motors. *Ultrasonics*, vol. 46, pp. 303-312.

Tsai, M.C. and Yao, W.S. (2002). Design of a plug-in type repetitive controller for periodic inputs. *IEEE Transactions on Control Systems Technology*, vol. 10, pp. 547-555.

Xu, X., Liang, Y.C., Lee, H.P., Lin, W.Z., Lim, S.P. and Shi, X.H. (2005). A stable adaptive neural-network-based scheme for dynamical system control. *Journal of Sound and Vibration*, vol. 285, pp. 653-667.